Cell Reports, Volume *37*

Supplemental information

Identification of RAS mutant biomarkers for EGFR inhibitor sensitivity using a systems biochemical approach

Thomas McFall and Edward C. Stites

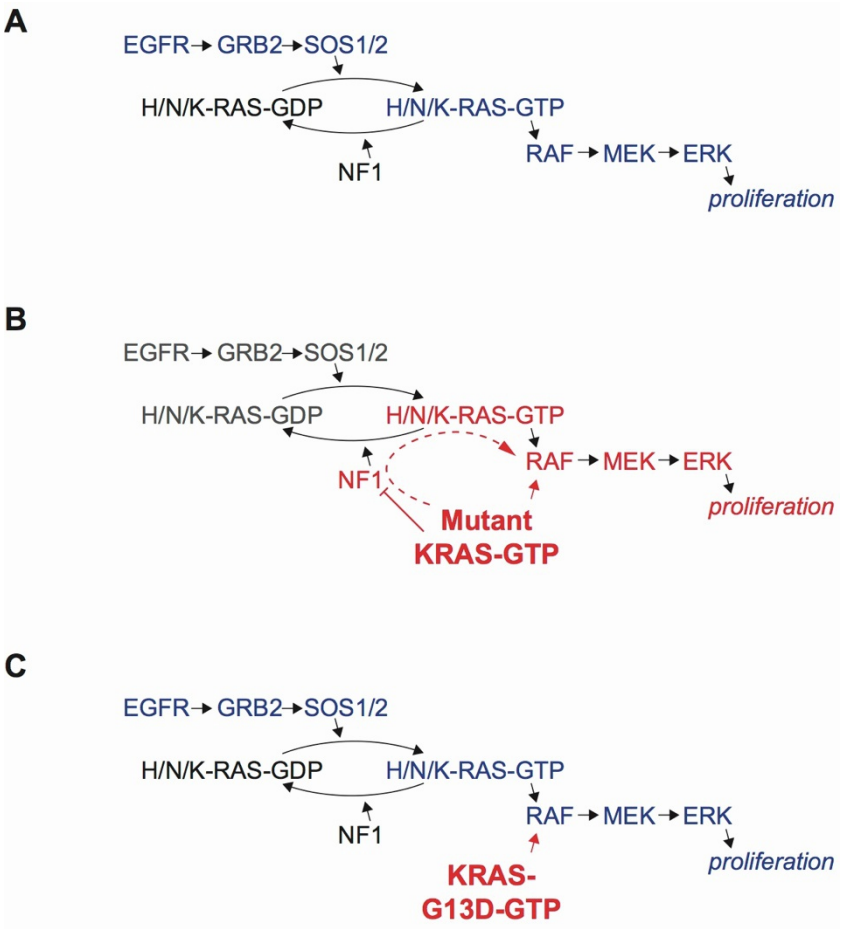

Figure S1

Figure S1. The mechanism of *KRAS* G13D sensitivity to EGFR inhibition that was uncovered in our previous work. Related to Figure 1. (**A**) The EGFR pathway leads to activation of the RAS GTPases (K/N/H-RAS) and the RAS downstream effector pathways, including the RAF/MEK/ERK MAPK cascade. (**B**) The most common constitutively active RAS mutations can activate the RAF/MEK/ERK cascade directly. Most RAS mutants can also indirectly active the RAF/MEK/ERK cascade by competitively inhibiting the RAS GAP and RAS signal negative regulator NF1. Decreased NF1 activity results in increased wild-type RAS-GTP activation that can also promote RAF/MEK/ERK activation. Both the direct and indirect activation of RAF/MEK/ERK signaling here occur in an EGFR independent manner. (**C**) KRAS G13D is constitutively active, but impaired at binding to NF1. Thus, it can partially activate the RAF/MEK/ERK cascade. Full activation of the RAF/MEK/ERK cascade (i.e. at a level comparable to KRAS G12V or KRAS G12D) requires another signal, like EGFR induction, to activate wild-type RAS-GTP.

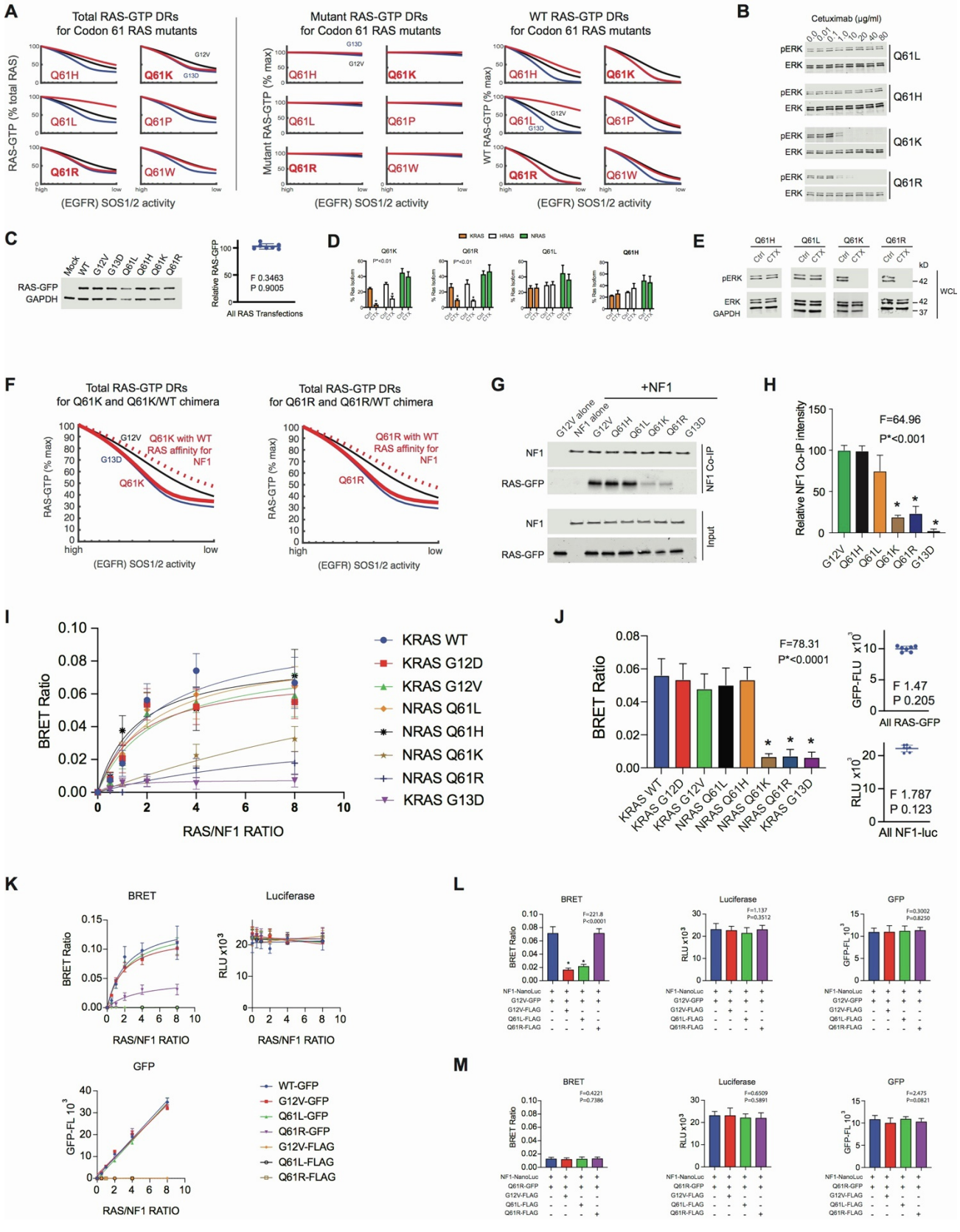
A
Total RAS-GTP DRs for Codon 61 RAS mutants
Mutant RAS-GTP DRs for Codon 61 RAS mutants
WT RAS-GTP DRs for Codon 61 RAS mutants
RAS-GTP (% total RAS)
Mutant RAS-GTP (% max)
WT RAS-GTP (% max)
Q61H
Q61K
Q61L
Q61P
Q61R
Q61W
G12V
G13D
(EGFR) SOS1/2 activity
B
Cetuximab (μg/ml)
0.0 0.01 0.1 1.0 10 20 40 80
pERK
ERK
C
Mock WT G12V G13D Q61L Q61H Q61K Q61R
RAS-GFP
GAPDH
Relative RAS-GFP
F 0.3463
P 0.9005
All RAS Transfections
D
KRAS HRAS NRAS
% Ras Isoform
Ctrl CTX
E
Ctrl CTX
kD
WCL
F
Total RAS-GTP DRs for Q61K and Q61K/WT chimera
Total RAS-GTP DRs for Q61R and Q61R/WT chimera
Q61K with WT RAS affinity for NF1
Q61R with WT RAS affinity for NF1
G
+NF1
G12V alone
NF1 alone
NF1
RAS-GFP
NF1 Co-IP
Input
H
Relative NF1 Co-IP intensity
F=64.96
P*<0.001
I
BRET Ratio
RAS/NF1 RATIO
KRAS WT
KRAS G12D
KRAS G12V
NRAS Q61L
NRAS Q61H
NRAS Q61K
NRAS Q61R
KRAS G13D
J
BRET Ratio
F=78.31
P*<0.0001
GFP-FLU x10³
F 1.47
P 0.205
All RAS-GFP
RLU x10³
F 1.787
P 0.123
All NF1-luc
K
BRET
Luciferase
GFP
WT-GFP
G12V-GFP
Q61L-GFP
Q61R-GFP
G12V-FLAG
Q61L-FLAG
Q61R-FLAG
L
F=221.8
P<0.0001
F=1.137
P=0.3512
F=0.3002
P=0.8250
M
F=0.4221
P=0.7386
F=0.6509
P=0.5891
F=2.475
P=0.0821

Figure S2

Figure S2. Supplementary investigations of the sensitivity of cells and networks with an *NRAS* codon 61 mutation to EGFR inhibition. Related to Figure 2. (**A**) Simulated dose responses for six codon 61 RAS mutants (red), compared to G13D (blue) and G12V (black) mutants. Measures of model output considered are total RAS-GTP (left), mutant RAS-GTP (middle), and wild-type RAS-GTP (right). (**B**) Immunoblots of *NRAS* Q61L, Q61H, Q61K and Q61R SW48 isogenic treated indicated doses of cetuximab (48 h). Experiment was performed once (N=1) to confirm MTT proliferation assay (Figure 2C). (**C**) Immunoblots of RAS mutant expression (left). Relative values of RAS-GFP were normalized to GAPDH, and ratios of RAS to GAPDH were further normalized to the WT RAS lane (100%) (right). Each data point represents the average expression across three separate experiments (N=3). One-way ANOVA was performed and no statistical difference in RAS expression across transfections was observed. (**D**) Quantification of RAS-GTP levels from RBD-IEF. Data points and error bars represent mean ± SD from three separate experiments (N=3), of which Figure 2G is a representative example. Statistical significance was determined with the unpaired two-tailed t-test. P* indicates a significance of <0.01. (**E**) ERK phosphorylation measurements made in parallel with the RBD-IEF experiment shown in Figure 2G. (**F**) Simulated EGFR (SOS) inhibition dose responses for Q61K and Q61R mutants with their measured affinity reduction for NF1 (red solid line), and with their impaired affinity replaced with the affinity of WT RAS for NF1 (red dashed line). Simulated dose responses for G13D (blue) and G12V (black) mutants are also presented. (**G**) Coimmunoprecipitation of NF1 with NRAS Q61H, Q61L, Q61K, Q61R and KRAS G13D and G12V from mixtures of lysates from *NF1*-transfected cells with lysates from *RAS*-transfected cells. Western blot is representative for three independent experiments (N=3). (**H**) Normalized densitometry from three independent NF1-CoIP. Data points and error bars represent mean ± SD amongst three independent experiments (N=3). Statistical difference was determined by one-way ANOVA followed by post-hoc Tukey's test for multiple comparisons. P* values indicate a significance of <0.001 when compared against KRAS G12V. (**I**) HEK293T cells were transfected with *NF1-NanoLuc* and with increasing concentrations of *RAS-GFP* at the ratio indicated. Data represents BRET ratio ± SD from eight biological replicates (n=8). BRET saturation curves are from one representative experiment from three independent experiments (N=3). (**J**) Data represent BRET ratio ± SD from eight biological replicates (n=8). BRET value is a single point from the BRET curve (Panel A) at a 2:1 concentration of *RAS-GFP*: *NF1-NanoLuc* expression constructs. Statistical difference was determined by one-way ANOVA followed by post-hoc Tukey's test for multiple comparisons. P* values indicate a significance of <0.0001 when compared against KRAS WT. The small distribution plots on the right show average luciferase and GFP fluorescence units, indicating equal amounts of NF1-NanoLuc and RAS-GFP expression across transfections. Each data point represents the average signal across eight biological replicates (n=8). One-way ANOVA was performed and no statistical difference was observed. (**K**) Flag-tagged and GFP-tagged KRAS proteins were analyzed for BRET signal with NF1-NanoLuc (top left). NF1-NanoLuc expression was held constant throughout the BRET saturation curve as indicated by equal levels of luciferase units (top right). Increasing levels of GFP signal correspond with an increasing quantity of *RAS-GFP* construct transfection (bottom left). (**L**) Evaluation of the ability of Flag-tagged KRAS G12V, Q61L, and Q61R to compete with KRAS G12V-GFP for binding to NF1 (left). Equal amounts of luciferase (middle) and GFP (right) were observed, suggesting equal amounts of expression that followed from the transfection of equal amounts of the respective constructs. Data represents the average signal ± SD across eight biological replicates (n=8), and are representative of three experiments (N=3). One-way ANOVA was performed followed by post-hoc Tukey's test for multiple comparisons. P- and F values are indicated. (**M**) Evaluation of the ability of Flag-tagged KRAS G12V, Q61L, and Q61R to compete with NRAS Q61R-GFP for binding to NF1(left). Equal amounts of luciferase (middle) and GFP (right) were observed, suggesting equal amounts of expression that followed from the transfection of equal amounts of the respective constructs. Data represents the average signal ± SD across eight biological replicates (n=8), and are representative of three experiments (N=3). One-way ANOVA was performed followed by post-hoc Tukey's test for multiple comparisons. P- and F values are indicated.

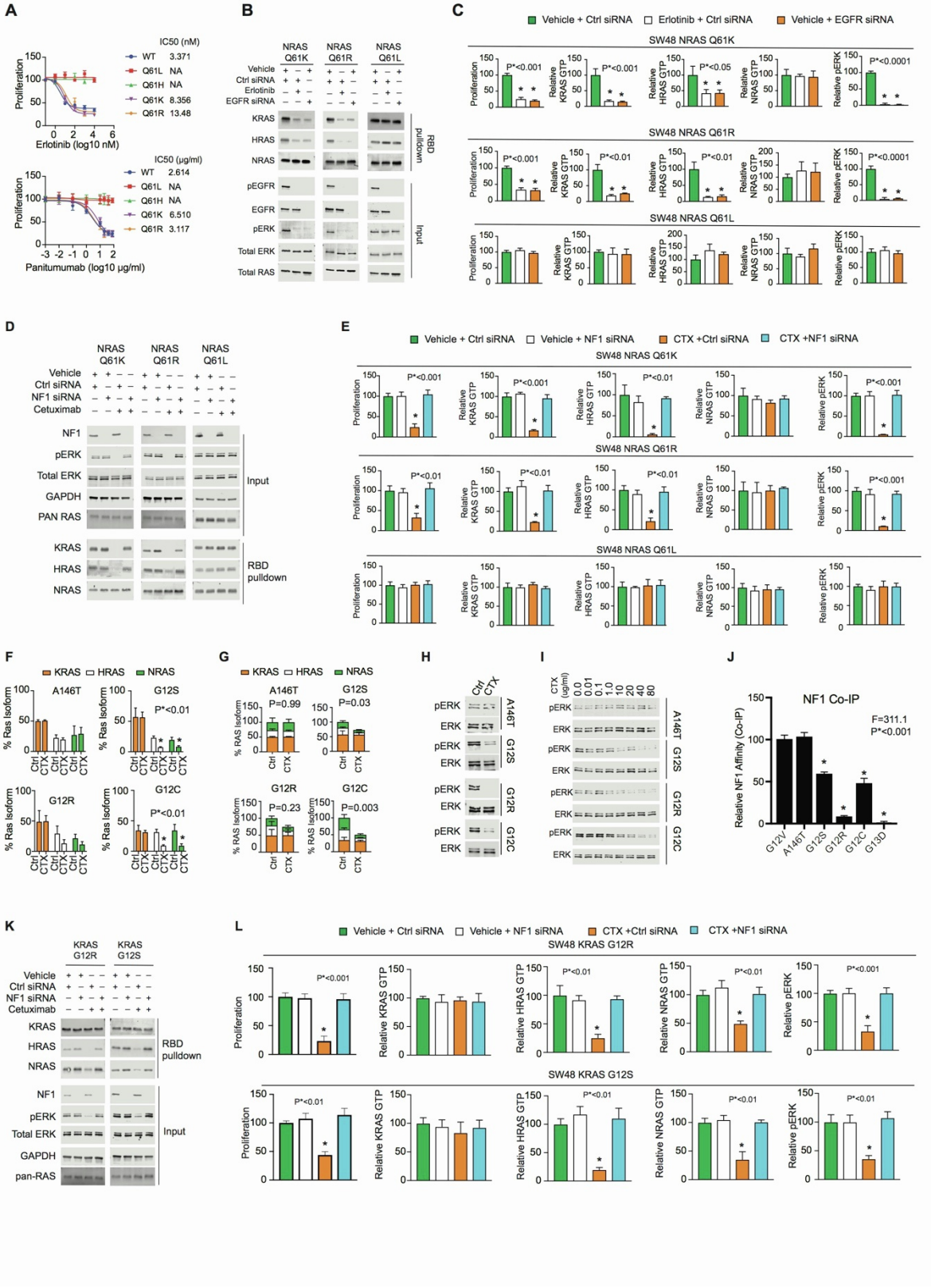
A
IC50 (nM)
WT 3.371
Q61L NA
Q61H NA
Q61K 8.356
Q61R 13.48
Proliferation
Erlotinib (log10 nM)
IC50 (μg/ml)
WT 2.614
Q61L NA
Q61H NA
Q61K 6.510
Q61R 3.117
Panitumumab (log10 μg/ml)
B
NRAS Q61K
NRAS Q61R
NRAS Q61L
Vehicle
Ctrl siRNA
Erlotinib
EGFR siRNA
KRAS
HRAS
NRAS
RBD pulldown
pEGFR
EGFR
pERK
Total ERK
Total RAS
Input
C
Vehicle + Ctrl siRNA
Erlotinib + Ctrl siRNA
Vehicle + EGFR siRNA
SW48 NRAS Q61K
SW48 NRAS Q61R
SW48 NRAS Q61L
Proliferation
Relative KRAS GTP
Relative HRAS GTP
Relative NRAS GTP
Relative pERK
P*<0.001
P*<0.05
P*<0.01
P*<0.0001
D
NRAS Q61K
NRAS Q61R
NRAS Q61L
Vehicle
Ctrl siRNA
NF1 siRNA
Cetuximab
NF1
pERK
Total ERK
GAPDH
PAN RAS
Input
KRAS
HRAS
NRAS
RBD pulldown
E
Vehicle + Ctrl siRNA
Vehicle + NF1 siRNA
CTX +Ctrl siRNA
CTX +NF1 siRNA
SW48 NRAS Q61K
SW48 NRAS Q61R
SW48 NRAS Q61L
Proliferation
Relative KRAS GTP
Relative HRAS GTP
Relative NRAS GTP
Relative pERK
P*<0.001
P*<0.01
F
KRAS
HRAS
NRAS
% Ras Isoform
A146T
G12S
G12R
G12C
P*<0.01
Ctrl
CTX
G
KRAS
HRAS
NRAS
% RAS Isoform
A146T
P=0.99
G12S
P=0.03
G12R
P=0.23
G12C
P=0.003
Ctrl
CTX
H
Ctrl
CTX
pERK
ERK
A146T
G12S
G12R
G12C
I
CTX (ug/ml)
0.0
0.01
0.1
1.0
10
20
40
80
pERK
ERK
A146T
G12S
G12R
G12C
J
NF1 Co-IP
Relative NF1 Affinity (Co-IP)
F=311.1
P*<0.001
G12V
A146T
G12S
G12R
G12C
G13D
K
KRAS G12R
KRAS G12S
Vehicle
Ctrl siRNA
NF1 siRNA
Cetuximab
KRAS
HRAS
NRAS
RBD pulldown
NF1
pERK
Total ERK
GAPDH
pan-RAS
Input
L
Vehicle + Ctrl siRNA
Vehicle + NF1 siRNA
CTX +Ctrl siRNA
CTX +NF1 siRNA
SW48 KRAS G12R
SW48 KRAS G12S
Proliferation
Relative KRAS GTP
Relative HRAS GTP
Relative NRAS GTP
Relative pERK
P*<0.001
P*<0.01

Figure S3

Figure S3. Empirical investigations of the sensitivity of *NRAS* and *KRAS* mutant isogenic SW48 cells to EGFR inhibition. Related to Figure 2 and Figure 3. (**A**) Drug dose response MTT assays for *NRAS* Q61K, Q61R, Q61L, and Q61H isogenic SW48 cells that were treated with erlotinib (top) or panitumumab (bottom). Data points represent mean ± SD. Dose response is representative of three independent experiments (N=3). (**B**) Immunoblots of whole cell lysates and RBD-pull down lysates for *NRAS* Q61K Q61R, and Q61L SW48 cells. (**C)** Quantifications of proliferation (MTT assay), RAS-GTP levels (immunoblot), and ERK phosphorylation (immunoblot) for *NRAS* Q61K, Q61R, and Q61L isogenic SW48 cells treated with erlotinib, *EGFR* siRNA, or control siRNA. Data points represent mean ± SD from three separate experiments (N=3), for which Figure S3B is a representative example of the immunoblots. Proliferation measurements for these same conditions were made separately and are presented here. Statistical significance was determined by performing one-way ANOVA followed by post-hoc Tukey's test for multiple comparisons between untreated and treated conditions. P values are indicated. (**D**) Immunoblots of whole cell lysates and RBD-pull down lysates for *NRAS* Q61K, Q61R, and Q61L genotype isogenic SW48 cells that were treated with cetuximab (or not) and also treated with *NF1* siRNA or control siRNA. (**E**) Quantification of isoform specific RAS-GTP levels from RBD pulldown, and of ERK phosphorylation. Proliferation measurements for these same conditions were made separately and are presented here. Data points represent mean ± SD from three separate experiments (N=3). Statistical difference was determined by one-way ANOVA followed by post-hoc Tukey's test for multiple comparisons. (**F**) Quantification of RAS-GTP levels RBD-IEF. Data points represent mean ± SD from three separate experiments (N=3), for which Figure 3C was a representative example. Statistical significance was determined by performing unpaired two-tailed t-test between untreated and treated conditions for each isoform specific RAS-GTP for each cell line. P* indicates a significance of <0.01. (**G**) RAS-GTP levels as a scaled fraction of total RAS-GTP from RBD-IEF. Data points represent mean ± SD from three separate experiments (N=3). Statistical significance was determined by performing unpaired two-tailed t-test between untreated and treated conditions for total RAS-GTP. P-values are indicated within the figure. (**H**) ERK phosphorylation measured in cetuximab treated and non-treated cells that was performed in parallel with the RBD-IEF measurements shown in Figure 3C. (**I**) Immunoblots of *KRAS* A146T, G12R, G12S and G12C SW48 isogenic cells were treated with increasing doses of cetuximab for 48h. Dose response western blot was performed once (N=1) to confirm MTT proliferation assay (Figure 3A). (**J**) Normalized densitometry from three independent NF1-CoIP experiments representing relative NF1 affinity *in vitro* from Figure 3D. Bar heights and error bars represent mean and standard deviation amongst three independent experiments (N=3). Statistical difference was determined by one-way ANOVA followed by post-hoc Tukey's test for multiple comparisons. P* indicate a significance of <0.001 when compared against KRAS G12V. (**K**) Immunoblots of whole cell lysates and RBD-pull down lysates for *KRAS* G12R and G12S isogenic SW48 cells that were treated with cetuximab (or not) and also treated with *NF1* or control siRNA. (**L**) Quantification of isoform specific RAS-GTP levels from RBD pulldown, and of ERK phosphorylation. Proliferation measurements for these same conditions were made separately and are also presented here. Data points represent mean ± SD from three separate experiments (N=3). Statistical difference was determined by one-way ANOVA followed by post-hoc Tukey's test for multiple comparisons.

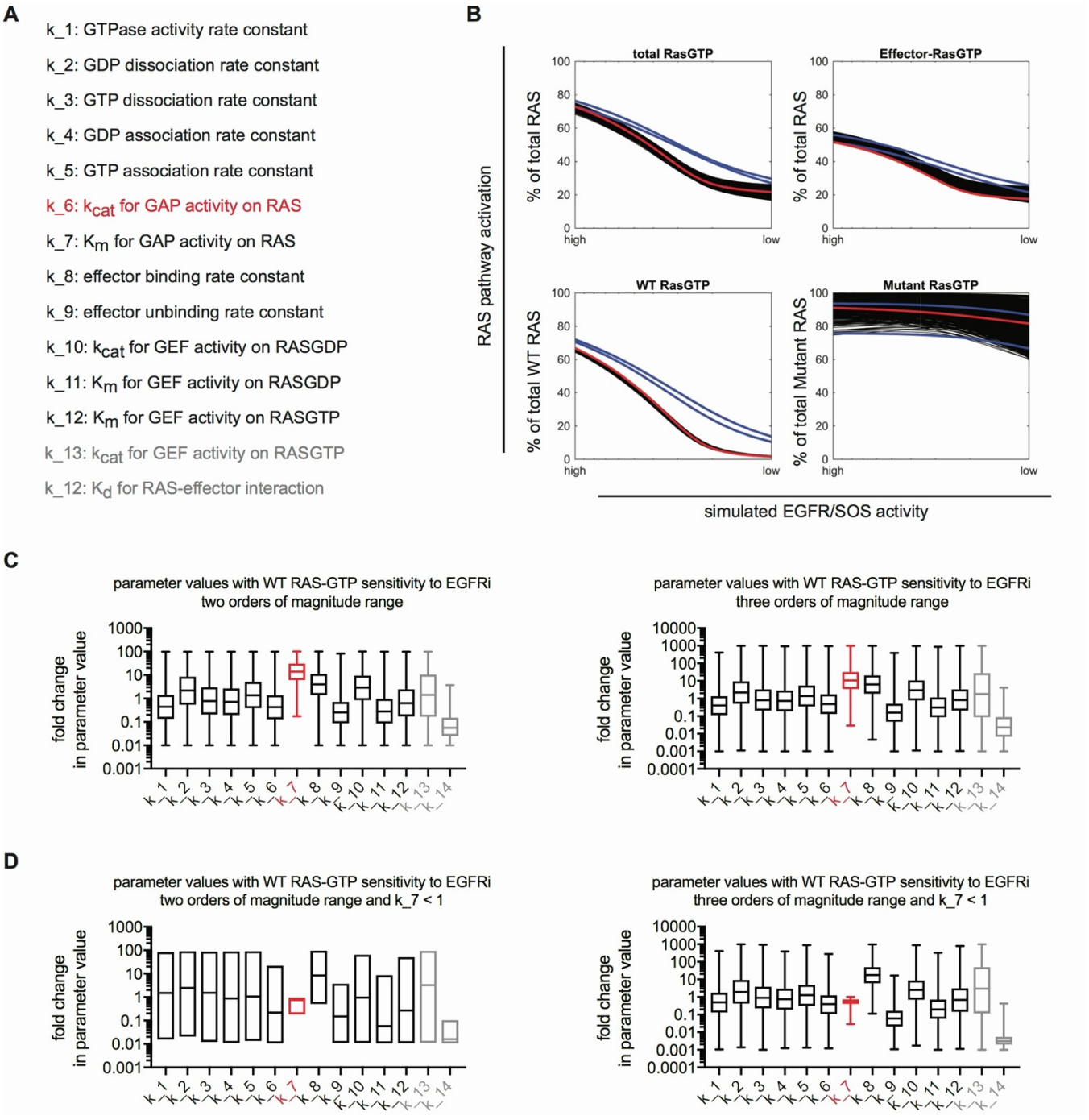
A
k_1: GTPase activity rate constant
k_2: GDP dissociation rate constant
k_3: GTP dissociation rate constant
k_4: GDP association rate constant
k_5: GTP association rate constant
k_6: kcat for GAP activity on RAS
k_7: Km for GAP activity on RAS
k_8: effector binding rate constant
k_9: effector unbinding rate constant
k_10: kcat for GEF activity on RASGDP
k_11: Km for GEF activity on RASGDP
k_12: Km for GEF activity on RASGTP
k_13: kcat for GEF activity on RASGTP
k_12: Kd for RAS-effector interaction
B
RAS pathway activation
total RasGTP
Effector-RasGTP
WT RasGTP
Mutant RasGTP
% of total RAS
% of total WT RAS
% of total Mutant RAS
high
low
simulated EGFR/SOS activity
C
parameter values with WT RAS-GTP sensitivity to EGFRi
two orders of magnitude range
three orders of magnitude range
fold change in parameter value
D
parameter values with WT RAS-GTP sensitivity to EGFRi
two orders of magnitude range and k_7 < 1
three orders of magnitude range and k_7 < 1

Figure S4

Figure S4. Computational analysis of possible mechanisms for EGFR inhibitor sensitivity within RAS mutant networks. Related to Figure 4. (**A**) Table providing definitions of each of the fourteen reaction parameters that characterize a RAS mutant within the RAS model. The K_m for the interaction between NF1 and a RAS mutant, which was found to be the most important parameter for determining whether a network is EGFRi sensitive, is indicated in red. The two parameters indicated in gray are dependent parameters that are composites of the other parameters. (**B**) Simulated EGFR/SOS inhibition dose responses (black lines) for all of the computational RAS mutants that are sensitive to EGFR inhibition within a collection of one million computational-random-RAS mutants where each of the RAS mutant parameters are within one order of magnitude from the parameter values of WT RAS for the same reaction. For comparison, the simulated dose response of G13D (red) and G12D and G12V (both blue) are presented. (**C**) Parameters from all of the parameter sets that resulted in EGFR inhibitor sensitivity through WT RAS-GTP reduction but not mutant RAS-GTP reduction. Parameters are presented normalized to the value of the same parameter for WT RAS. These data are like the data in Figure 4F, but for a collection of one million computational-random-RAS mutants where each of the RAS mutant parameters is within two orders of magnitude from the parameter value of WT RAS (left) or within three orders of magnitude (right). (**D**) Parameters from all of the parameter sets in Figure S8C, but further limited to those parameter sets that also have a K_m value for the NF1 interaction with mutant RAS that was less than the value of the K_m between NF1 and WT RAS.

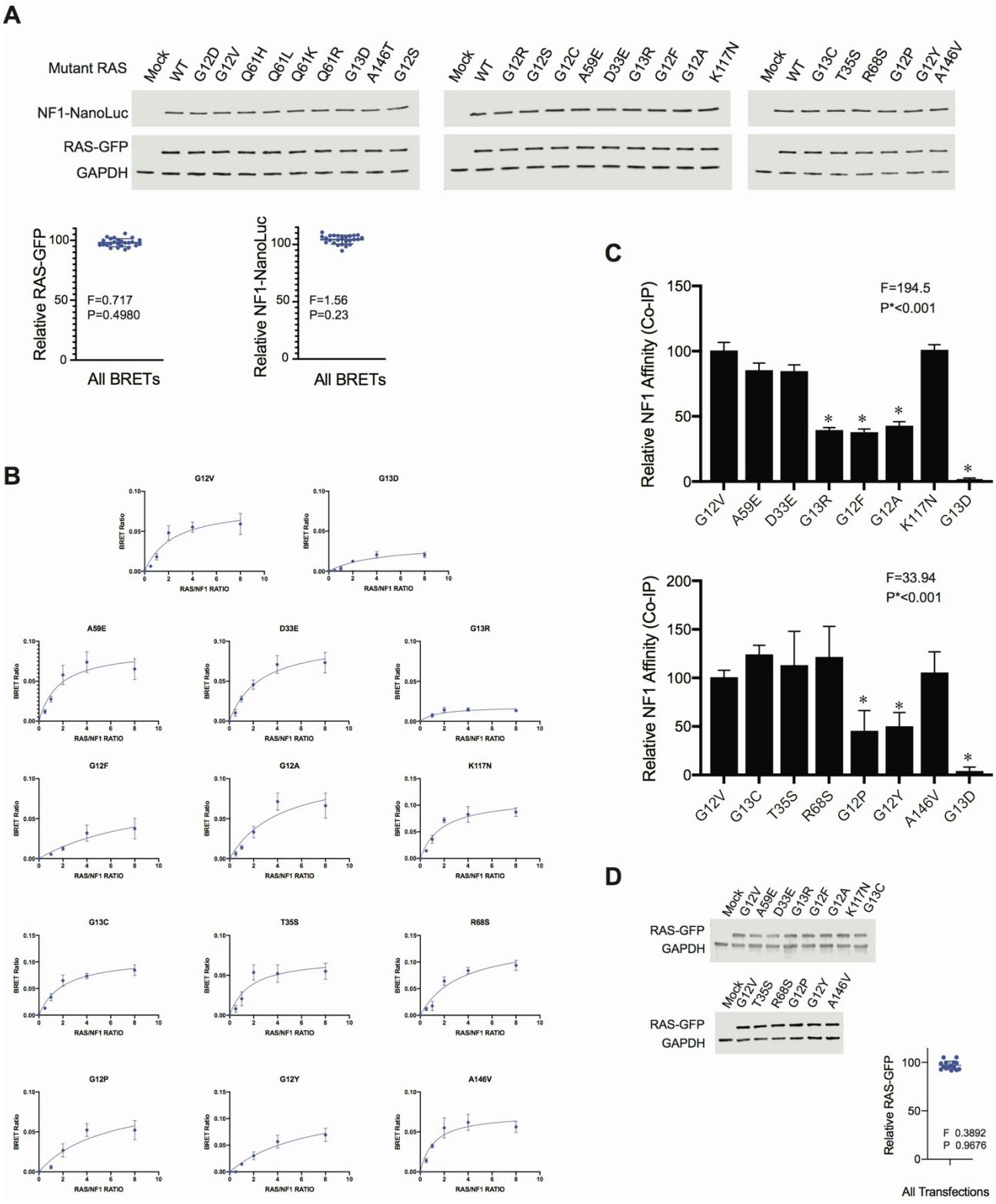
A
Mutant RAS
Mock WT G12D G12V Q61H Q61L Q61K Q61R G13D A146T G12S
Mock WT G12R G12S G12C A59E D33E G13R G12F G12A K117N
Mock WT G13C T35S R68S G12P G12Y A146V
NF1-NanoLuc
RAS-GFP
GAPDH
Relative RAS-GFP
F=0.717
P=0.4980
All BRETs
Relative NF1-NanoLuc
F=1.56
P=0.23
All BRETs
B
G12V
G13D
A59E
D33E
G13R
G12F
G12A
K117N
G13C
T35S
R68S
G12P
G12Y
A146V
BRET Ratio
RAS/NF1 RATIO
C
Relative NF1 Affinity (Co-IP)
F=194.5
P*<0.001
G12V A59E D33E G13R G12F G12A K117N G13D
F=33.94
P*<0.001
G12V G13C T35S R68S G12P G12Y A146V G13D
D
Mock G12V A59E D33E G13R G12F G12A K117N G13C
RAS-GFP
GAPDH
Mock G12V T35S R68S G12P G12Y A146V
RAS-GFP
GAPDH
Relative RAS-GFP
F 0.3892
P 0.9676
All Transfections

Figure S5

Figure S5. Supplementary data from the empiric screening of twelve KRAS mutants for binding to NF1. **Related to Figure 5.** (**A**) Evaluation of KRAS expression after HEK-293T cells were transfected with same quantity of DNA for the indicated *RAS-GFP* and *NF1-NanoLuc* constructs. KRAS-GFP expression was normalized to GAPDH as an internal protein loading control and to the WT-lane (100%) for an external reference to compare across western blots. RAS-GFP expression from the three western blots show little variation and each data point represents RAS expression for each mutant (bottom left). Mean and standard deviation of expression from all RAS-GFP transfections from within each western blot were calculated, one-way ANOVA was performed, and no statistical difference in expression was observed in RAS-GFP expression across western blots (bottom left). NF1-NanoLuc expression was normalized to GAPDH as an internal protein loading control, and to the WT-lane for an external reference (100%) to compare expression across western blots. NF1-NanoLuc expression from the three western blots show little variation (bottom left). Mean and standard deviation of expression from all NF1-NanoLuc transfections from each western blot were calculated, one-way ANOVA was performed, and no statistical difference in expression was observed across western blots (bottom left). P- and F-Values are reported for comparison. Each western blot was performed once (N=1). (**B**) Full BRET saturation curves that provided the source data for Figure 5B (2:1 RAS:NF1 transfection ratio). HEK293T cells were transfected with NF1-NanoLuc and with increasing concentrations of the indicated *RAS-GFP* construct. BRET curves for KRAS G12V and KRAS G13D, which have previously been shown to display approximately wild-type levels of NF1 binding and reduced NF1 binding, respectively, are included for comparison. Data represent BRET ratio ± SD from eight biological replicates (n=8) BRET saturation curves are a single representative experiment of three independent experiments (N=3). (**C)** Normalized densitometry from three independent NF1-CoIP experiments representing relative NF1 affinity *in vitro,* of which Figure 5C is one representative example. Bar heights represent mean ± SD amongst three independent experiments (N=3). Statistical difference was determined by one-way ANOVA followed by post-hoc Tukey's test for multiple comparisons. P* indicate a significance of <0.001 when compared against KRAS G12V. (**D)** Evaluation of RAS expression after SW48 *WT* cells were transfected with same quantity of mutant *RAS-GFP* constructs pertaining to Figure 5B. RAS-GFP expression was normalized to GAPDH for internal protein loading control and to G12V-RAS-GFP (100%) for an external reference to compare across western blots. Each data point on the distribution plot represents mean expression of each mutant RAS from three separate experiments (N=3). One-way ANOVA was performed to compare all mutants against each other, and no significant difference was observed as reported by P- and F- values.

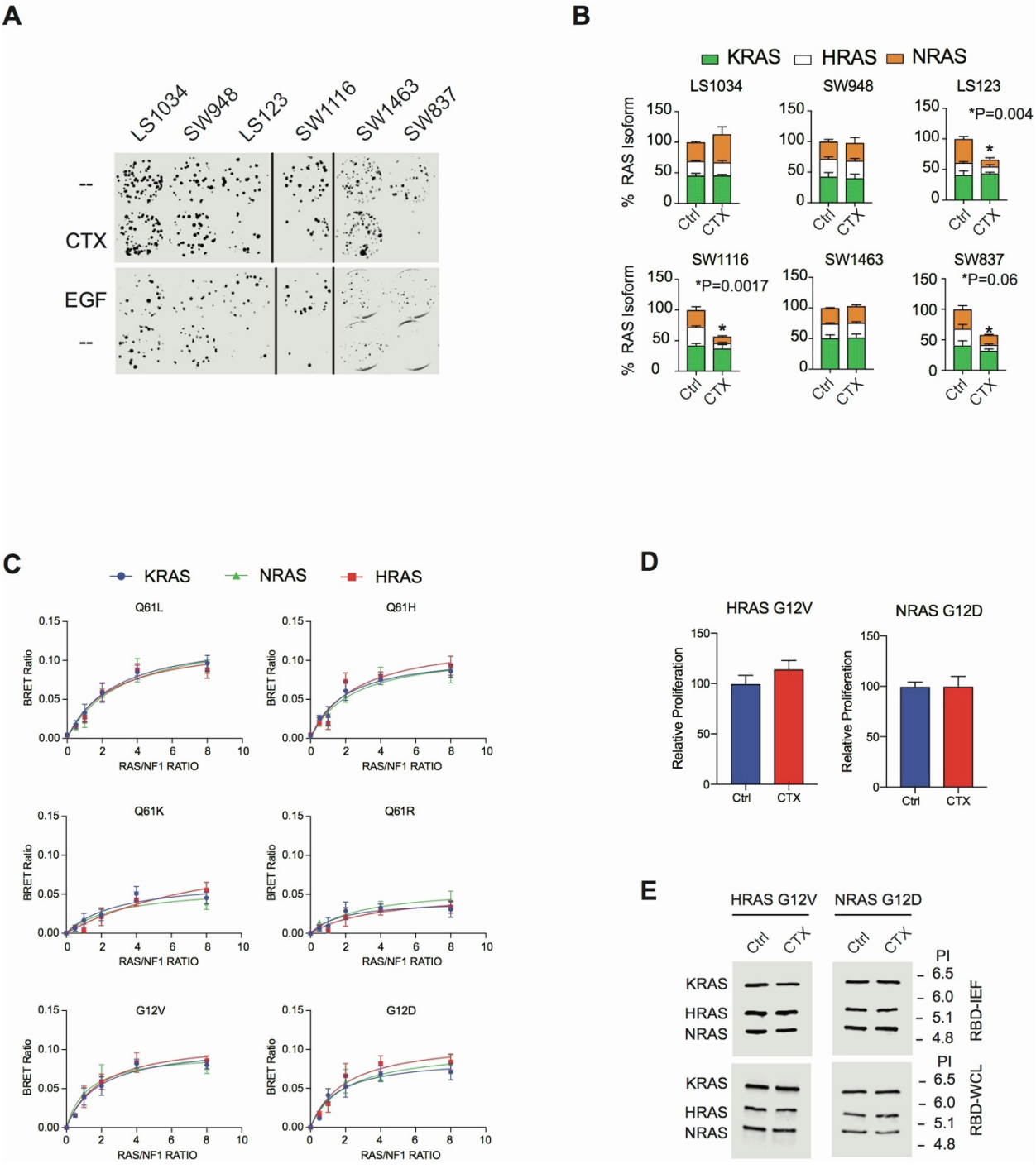
A
LS1034
SW948
LS123
SW1116
SW1463
SW837
--
CTX
EGF
--
B
KRAS
HRAS
NRAS
LS1034
SW948
LS123
*P=0.004
SW1116
*P=0.0017
SW1463
SW837
*P=0.06
% RAS Isoform
Ctrl
CTX
C
KRAS
NRAS
HRAS
Q61L
Q61H
Q61K
Q61R
G12V
G12D
BRET Ratio
RAS/NF1 RATIO
D
HRAS G12V
NRAS G12D
Relative Proliferation
Ctrl
CTX
E
HRAS G12V
NRAS G12D
Ctrl
CTX
KRAS
HRAS
NRAS
PI
6.5
6.0
5.1
4.8
RBD-IEF
RBD-WCL

Figure S6

Figure S6. Supplementary data from the validation of identified EGFR inhibitor sensitive *RAS* mutants in additional model systems and *RAS* genes. Related to Figure 6. (**A**) Colony formation assays for LS1034, SW1116, LS123, SW948, SW837 and SW1463 cells. Images are one representative experiment of three independent experiments (N=3). **(B)** Quantification of isoform specific RAS-GTP level from RBD-IEF. Data points and error bars represent mean ± SD from three separate experiments (N=3), for which Figure 6C is a representative example. Statistical significance was determined by performing unpaired two-tailed t-test between untreated and treated conditions for each genotype. P* indicates a significance of <0.05. (**C**) HEK293T cells were transfected with *NF1-NanoLuc* and with increasing concentrations of the indicated mutant *RAS-GFP*. Data represent BRET ratios ± SD from eight biological replicates (n=8). BRET saturation curves are from one representative experiment. Three independent experiments were performed (N=3). (**D**) Proliferation assays for *HRAS* G12V and *NRAS* G12D SW48 isogenic cells. Data points represent mean ± SD, and are representative of three separate experiments (N=3). (**E**) RBD-IEF and WCL-IEF of *HRAS* G12V and *NRAS* G12D SW48 isogenic cells cultured in untreated or treated conditions (20 µg/ml of cetuximab for 48 hours). RBD-IEF and WCL-IEF are each representative of three independent experiments (N=3).